

Interaction of Dicationic Bis(imidazoliumyl)porphyrinatometals with DNA

Tomoko Yamamoto, Daryono Hadi Tjahjono,# Naoki Yoshioka, and Hidenari Inoue*

Department of Applied Chemistry, Keio University, 3-14-1 Hiyoshi, Kohoku-ku, Yokohama 223-8522

Received March 24, 2003; E-mail: inoue@applc.keio.ac.jp

A pair of dicationic metalloporphyrins with only two *meso*-substituents, i.e. copper(II) and zinc(II) complexes of 5,15-bis(1,3-dimethylimidazolium-2-yl)porphyrin (H_2-**1**), have been synthesized by insertion reaction of the metal ions. Interactions of [5,15-bis(1,3-dimethylimidazolium-2-yl)porphyrinato]copper(II) (Cu-**1**) and [5,15-bis(1,3-dimethylimidazolium-2-yl)porphyrinato]zinc(II) (Zn-**1**) with calf thymus DNA (CT-DNA) and double-helical synthetic polynucleotides ($[poly(dA–dT)]_2$ and $[poly(dG–dC)]_2$) have been studied by melting temperature, viscometric, visible absorption, CD and MCD spectroscopic measurements. The copper(II) complex, Cu-**1**, intercalates into the base pairs of DNA such as CT-DNA, $[poly(dA–dT)]_2$ and $[poly(dG–dC)]_2$ to stabilize the DNA duplex due to its high affinity for them. In contrast, the zinc(II) complex, Zn-**1**, binds edge-on to CT-DNA, $[poly(dA–dT)]_2$ and $[poly(dG–dC)]_2$ as an outside binder. The binding constant of Cu-**1** to DNA is in the order of 10^6 M^{-1} in a phosphate buffer (pH 6.8) at 25 °C, while that of Zn-**1** ranges from 10^4 to 10^5 M^{-1} under the same experimental conditions. The binding of Cu-**1** and Zn-**1** to DNA is entropically driven, although that of H_2-**1** is enthalpically driven. As a result, it has been revealed that the kind of central metal ions in dicationic metalloporphyrins influences the binding properties of the dicationic porphyrin to DNA.

The macrocyclic molecules with the skeletal structure of porphyrins have received much attention because of their essential role in biological systems. The porphyrins have very strong absorption in the visible region due to their characteristic macrocycle, such that their solution properties and DNA binding have been extensively studied by spectroscopic methods.[1,2] In particular, cationic porphyrins and their non-covalent interactions with DNA are of importance from the viewpoint of their potential therapeutic use as a photosensitizer in photodynamic therapy (PDT) and as a DNA cleaver.[3,4] It is generally accepted that the binding of cationic porphyrins to DNA occurs in two steps.[5] First, the access of the porphyrin to DNA is driven by electrostatic interaction between the positively charged substituent on the porphyrin periphery and the negatively charged phosphate oxygen atom of DNA. Second, the molecular plane of the porphyrin enters between the base pairs of DNA to stabilize the porphyrin–DNA complex by favorable aromatic π–π interaction between the porphyrin macrocycle and the base pair of nucleic acid. Three major binding modes have been proposed for the binding of cationic porphyrins to DNA: intercalation, outside groove binding, and outside binding with self-stacking in which cationic porphyrins are stacked along the DNA helix.[6,7] The single-crystal study of a cationic porphyrin–oligonucleotide complex has revealed that the intercalation or hemiintercalation of cationic porphyrins into DNA requires a conformational distortion of DNA.[8]

The nature of porphyrins also plays an important role in their binding to DNA, in addition to the experimental conditions such as pH, ionic strength, and the molar ratio of [porphyrin]/[DNA in base pair]. Therefore, design and synthesis of new cationic porphyrins are indispensable for studies of their interaction with DNA.[9] In the past decade *meso*-tetrakis(4-*N*-methylpyridiniumyl)porphyrin (H_2TMPyP) and its derivatives have become the well-known tetracationic porphyrins with six-membered rings at the *meso*-position, and their interaction with DNA has been intensively studied.[10,11] Recently, it has been reported that tetracationic porphyrins with five-membered rings as *meso*-substituents interact with DNA.[12] Their DNA-binding properties are different from those of well-known H_2TMPyP due to the difference in charge distribution or electron density of *meso*-substituents. In the previous work, we have focused on the π–π interaction as a driving force in the DNA binding, and on dicationic porphyrins with two imidazolium rings at the 5,15-position (H_2-**1**).[13] The π electronic system effective for DNA binding is widely extended or more naked in H_2-**1** compared to that of the porphyrins with four substituents at the *meso*-position (Fig. 1). In fact, the absence of two *meso*-substituents at the *trans*-position facilitates the intercalation of the porphyrin into the DNA base pairs, even into the A–T base pairs. On the other hand, there have been a num-

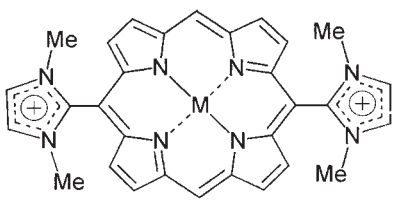

Fig. 1. Structure of 5,15-bis(imidazolium-2-yl)porphyrinatometals. M is H_2, Cu^{II} or Zn^{II}.

On sabbatical leave from Department of Pharmacy, Bandung Institute of Technology, Jalan Ganesha 10, Bandung 40132, Indonesia

Published on the web October 15, 2003; DOI 10.1246/bcsj.76.1947

ber of intensive studies on interactions between tetracationic metalloporphyrin and DNA.[14] It has also been reported that the binding mode of tetracationic porphyrins to nucleic acid duplexes can be easily tuned by varying the metal center.[15] According to these reports, the thin square planar copper(II), palladium(II) and platinum(II) complexes of H_2TMPyP are capable of intercalation into the pocket between two adjacent, closely spaced (3.4 Å) base pairs of B-DNA. However, the manganese(III), iron(III), zinc(II), and cobalt(II) complexes of H_2TMPyP can bind only to the outside of the DNA duplex due to one or two axial ligands.

In light of the influence of the central metal ion on interaction of tetracationic metalloporphyrins with DNA, it is very attractive to study how the metal insertion into H_2-**1** changes the binding properties of dicationic porphyrins to nucleic acid duplexes, or how the central metal ion inserted affects the thermodynamic properties of interaction between dicationic porphyrin and DNA. It is particularly interesting to learn whether relatively small H_2-**1** can intercalate into the A–T base pairs upon inserting zinc(II) ions with A–T selectivity into H_2-**1**, and whether H_2-**1** selective to A–T can be changed in selectivity from A–T to G–C by insertion of copper(II) ions or not. In the present work, we describe the DNA-binding properties such as binding mode, binding affinity, and thermodynamic parameters of dicationic porphyrin–DNA interaction, as well as the influence of the kind of central metal ions, i.e. copper(II) and zinc(II) ions, on the interaction between dicationic bisimidazoliumporphyrin and DNA.

Experimental

Materials and Instruments. Copper(II) chloride dihydrate and zinc(II) chloride were purchased from Wako Pure Chemical Industries, Ltd. and Kanto Chemical Co. Ltd., respectively. Ion exchange resin (CR-20) was supplied by Mitsubishi Chemical Co. Ltd. Calf thymus DNA (CT-DNA) and duplex synthetic DNA ($[poly(dA–dT)]_2$ and $[poly(dG–dC)]_2$) were obtained from Sigma Co. Ltd. and used as received. Other chemicals were used as received without further purification and all solvents were of reagent grade. The metal-free 5,15-bis(1,3-dimethylimidazolium-2-yl)porphyrin (H_2-**1**) was synthesized according to the previous method.[13] The UV–visible spectra were recorded in solution at 25 °C on a JASCO V-570 spectrophotometer equipped with a JASCO ETC-505T temperature controller using 10 mm quartz cells. The circular dichroism (CD) and magnetic circular dichroism (MCD) spectra were measured with a JASCO J-720 WI spectropolarimeter using 10 mm quartz cells. The ^{1}H NMR spectra were taken at 300 MHz with a JNM-LA300 spectrometer. Elemental analyses were performed at the Central Laboratory of the Faculty of Science and Technology, Keio University.

Synthesis of Bis(imidazoliumyl)porphyrinatometals. An aqueous solution of H_2-**1** (0.05 mmol) dissolved in water (30 cm^3) was stirred at room temperature for 30 min and filtered into a reflux flask. A solution of appropriate metal salt (0.1 mmol) in 10 cm^3 water was then added to the filtrate. The metal salts used in the present study were $CuCl_2 \cdot 2H_2O$ and $ZnCl_2$. The reaction mixture was then refluxed until no further change in the absorption peak of the Q band was observed. It took only one hour until four peaks became two persistent peaks. The solution was then cooled in an ice bath, allowed to stand overnight at room temperature, and filtered. The filtrate was then passed through an ion exchange resin (free base of polyamine). Drying of the precipitate under vacuum afforded bis(imidazoliumyl)porphyrinatometals.

Cu-**1** (red purple solid, 58%): Vis (phosphate buffer, pH 6.8, $\mu = 0.2$ M) λ_{max}/nm ($\log \varepsilon$) 401.0 (5.19), 531.0 (3.90), 567.0 (4.20), (Elemental analysis for $CuC_{30}H_{26}N_8I_2 \cdot 8H_2O$ requires C, 41.27; H, 4.83; N, 12.54%. Found: C, 41.48; H, 4.87; N, 12.90%); mp > 300 °C.

Zn-**1** (dark purple solid, 51%): ^{1}H NMR (300 MHz, DMSO-d_6; Me_4Si) δ 3.26 (s, 12H, imidazole-*N*-CH_3), 7.90 (s, 4H, imidazole-H), 8.54–8.56 (d, 4H, pyrrole-βH), 9.17–9.19 (d, 4H, pyrrole-βH), 10.03 (s, 2H, *meso*-H); Vis (phosphate buffer, pH 6.8, $\mu = 0.2$ M) λ_{max}/nm ($\log \varepsilon$) 407.5 (5.35), 541.0 (4.05), 573.5 (4.32), (Elemental analysis for $ZnC_{30}H_{26}N_8I_2 \cdot 5H_2O$ requires C, 45.98; H, 4.88; N, 13.52%. Found: C, 45.61; H, 4.71; N, 14.18%); mp > 300 °C.

Measurements of Viscosity and Melting Temperature (T_m). The viscosity of DNA solutions was measured at 30 ± 1 °C in a temperature-controlled circulating water-bath using a Ubbelohde viscometer. Typically, 10.0 cm^3 of phosphate buffer was transferred to the viscometer to obtain the reading of flow time. For the determination of solution viscosity, 10.0 cm^3 of 45 μM DNA in phosphate buffer was taken to the viscometer and a flow time reading was obtained. An appropriate amount of porphyrin in a buffered solution was then added to the viscometer to give a certain R value (= [porphyrin]/[DNA in base pair]) while keeping the DNA concentration constant, and the flow time was read. The flow time of samples was measured after the thermal equilibrium of the viscometer was achieved (ca. 60 min). Each point measured was the average of at least five readings with a relative standard deviation of less than 1%. The data obtained were presented as (η/η_O) versus R, where η is the reduced specific viscosity of DNA in the presence of porphyrin and η_O is the reduced specific viscosity of DNA alone.[16,17] The melting curves of both free DNA and the porphyrin–DNA complex in phosphate buffer were obtained by measuring the hyperchromicity of DNA at 260 nm as a function of temperature. Melting temperatures were measured in 45 μM DNA in phosphate buffer at pH 6.8 ($\mu = 0.2$ M NaCl). The temperature was scanned from 25 to 95 °C at a speed of 2 °C per min. The melting temperature (T_m) was taken as the mid-point of the hyperchromic transition. All measurements of T_m were repeated three times and the data presented are the average values with an RSD of lower than 5%.

Measurements of Spectra. All measurements, except where specifically indicated, were performed at 25 °C in a phosphate buffer (pH 6.8). The buffer solution consists of 6 mM Na_2HPO_4, 2 mM NaH_2PO_4, 1 mM EDTA, and a sufficient amount of NaCl to give a final ionic strength of $\mu = 0.2$ M. A stock solution of CT-DNA was prepared and stored in phosphate buffer. The extinction coefficients of $\varepsilon_{260} = 1.31 \times 10^4$ $M^{-1}\,cm^{-1}$ for CT-DNA,[18] $\varepsilon_{254} = 1.68 \times 10^4$ $M^{-1}\,cm^{-1}$ for $[poly(dG–dC)]_2$[19] and $\varepsilon_{262} = 1.32 \times 10^4$ $M^{-1}\,cm^{-1}$ for $[poly(dA–dT)]_2$[20] were used to determine their concentrations in base pair. The concentrations of the porphyrins were determined spectrophotometrically with $\varepsilon_{394} = 1.32 \times 10^5$ $M^{-1}\,cm^{-1}$ for H_2-**1**,[13] $\varepsilon_{400} = 1.56 \times 10^5$ $M^{-1}\,cm^{-1}$ for Cu-**1**, and $\varepsilon_{406} = 2.24 \times 10^5$ $M^{-1}\,cm^{-1}$ for Zn-**1**. The visible absorption spectra were measured by a JASCO V-570 spectrophotometer at a spectral band pass of 1 nm with 0.1 nm spectral resolution. The calibration of wavelength was carried out using a holmium oxide-glass standard. Induced CD spectra were obtained on a JASCO J-720 WI spectropolarimeter. Wavelength and intensity calibrations were performed using a 0.060% (w/v) aqueous solution of ammonium (1*S*)-camphor-10-sulfonate

(Aldrich). The CD spectra were recorded with the following instrument parameter settings: bandwidth; 2.0 nm, response time; 2.0 s, step resolution; 0.5 nm, and scan speed; 50 nm min^{-1} between 350 and 500 nm. The MCD spectra were also measured on a JASCO J-720 WI spectropolarimeter equipped with a JASCO MCD-317 water-cooled electromagnet and magnetic shielding of the detector. Wavelength and intensity were ascertained by 1.0 mM aqueous solutions of $K_3[Fe(CN)_6]$ and (+)-$[Co(en)_3]Cl_3$. The MCD spectra were measured in an applied magnetic field of $H = 1.1$ T and in the instrument parameter settings which are the same as those of CD spectral measurements. Total MCD spectra, [CD + MCD], were recorded in solution for free and DNA-bound porphyrin. Each MCD recording was preceded by a CD recording ($H_0 = 0.0$ T) of the sample in order to obtain the pure, net MCD spectra, i.e. net MCD = [CD + MCD] − [CD]. Typically, the porphyrin was titrated by stepwise addition of the stock solution of DNA directly to 2.5 cm^3 of starting volume of the porphyrin solution. Visible, induced CD and MCD spectra were measured successively.

In the interpretation of induced CD and MCD spectra, the porphyrin molecule is placed in the *xy*-plane and the inner hydrogen–hydrogen axis of the porphyrin is set to the *x*-axis while the other inner *N–N* axis is to the *y*-axis. For the bis(imidazoliumyl)porphyrinatometal, each of the inner *N–N* axes is set to the *x*- and *y*-axis. The two electric dipole transition moments (edtm, μ_e) of the porphyrin are in the direction of each axis. On the basis of the Weiss model,[21] μ_{ex} is the most perturbed direction, while μ_{ey} is the least perturbed direction. The CD results calculated by the CD matrix method,[22,23] which is abbreviated as CD-mm and supported by other approaches,[24,25] were used to interpret the CD spectra and to assess the binding mode of the porphyrin to DNA. The parameters α, θ, β and γ define the position and orientation of the porphyrin molecule relative to DNA (Fig. 2). The *X* axis in the coordinate system of DNA extends from the minor groove and constitutes a true C_2 axis of the B-DNA helix. In outside groove binding, the parameter α is the angle of edtm of the porphyrin with respect to the DNA helix axis (*Z*); θ is the azimuthal angle between the *X* axis and the line connecting the edtm of the porphyrin; β is the azimuthal angle between the line from the helix axis to the position of the edtm of the porphyrin and the projection of the edtm of the porphyrin onto the plane perpendicular to the helix axis and containing the same line. In intercalation, γ is the angle from the *X* axis to the edtm of the porphyrin in the *X–Y* plane of the intercalation pocket; *X*, *Y* and *Z* axes are defined as a right-handed Cartesian coordinate system (for detail, see Ref. 22–25). In addition, the MCD results were used to confirm the binding mode by comparing the excited state angular momenta (L_j), which are proportional to $[\Delta\theta]^{p-t}/\varepsilon_{max}$ of free and DNA-bound porphyrins, i.e., the energy differences in the π- and π^*-MOs ($1a_{1u}$ $3a_{2u}$ $4e_g$) of porphyrins.[26]

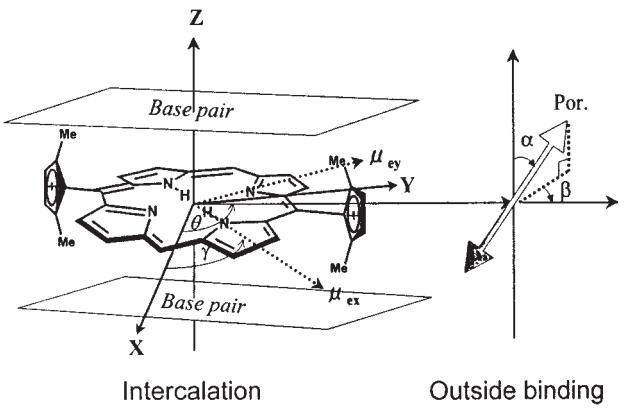

Fig. 2. Schematic of the intercalation and outside binding of the porphyrin to B-DNA.

Binding constants for the interaction of cationic porphyrins with DNA were determined by absorption spectrophotometric titration at a certain temperature. The fixed amount of cationic porphyrin in phosphate buffer was titrated at a certain temperature with the stock solution of DNA. The changes in absorbance of the Soret band upon addition of DNA were monitored at the maximum wavelength of the Soret band. The apparent binding constant, K_{app}, of cationic porphyrins to DNA was calculated by Eq. 1

$$[DNA]_{total}/(|\varepsilon_{app} - \varepsilon_f|) = \{1/(|\varepsilon_b - \varepsilon_f|)\}[DNA]_{total} + 1/\{K_{app}(|\varepsilon_b - \varepsilon_f|)\} \quad (1)$$

where ε_{app}, ε_f and ε_b correspond to A_{obsd}/[porphyrin], the extinction coefficient for the free porphyrin and that for the porphyrin in the fully bound form, respectively. In the plot of $[DNA]_{total}/(|\varepsilon_{app} - \varepsilon_f|)$ versus $[DNA]_{total}$, K_{app} is given by the ratio of the slope to the intercept.[27–29] The thermodynamics of porphyrin–DNA interaction was studied by means of the binding constants determined in the temperature range from 25 to 39 °C.

Results and Discussion

Physicochemical Evidence for Metalloporphyrin–DNA Interactions. The melting temperature (T_m) of DNA reflects the stability of the double helix of DNA and thus depends on the binding properties of porphyrin to DNA. Upon heating CT-DNA in a buffer solution, the A–T base pair having two hydrogen bonds is dissociated first and then the G–C base pair with three hydrogen bonds is cleaved, so that the double helix of DNA turns finally into two single stands. Since CT-DNA used in the present work is known to consist of 42% G–C base pair and 58% A–T base pair, measurements of the T_m in porphyrin solutions can explore the interaction between porphyrin and CT-DNA. In fact, the T_m of DNA has been used as an indicator of the binding properties of porphyrins to DNA,[30] although a comparative discussion of T_m should be restricted only to the data in the same binding mode. For this reason, the changes in the T_m, which were caused by the increasing addition of H_2-**1**, Cu-**1** or Zn-**1** to the phosphate buffer solution of CT-DNA, were measured in the range of *R* ([porphyrin]/[DNA in base pair]) = 0–0.25. Plots of the increase in melting temperature (ΔT_m) vs *R* are shown for H_2-**1**, Cu-**1** and Zn-**1** in Fig. 3. The T_m of CT-DNA is monotonously increased with the addition of H_2-**1**, Cu-**1** or Zn-**1** to the buffer solution of CT-DNA. The above results have shown that all the porphyrins studied interact with CT-DNA to stabilize the duplex structure irrespective of their binding mode. The insertion of the metal ions into H_2-**1** leads to an increase in ΔT_m, suggesting that at least the interaction between A–T or G–C base pairs is more enhanced by the metalloporphyrin than by the metal-free porphyrin. It is also noteworthy that the T_m of Cu-**1** is larger than that of H_2-**1** and thus Cu-**1** stabilizes the double helix more than H_2-**1**. This remarkable feature does not come from the difference in the binding mode but from that in the binding strength as described later in detail.

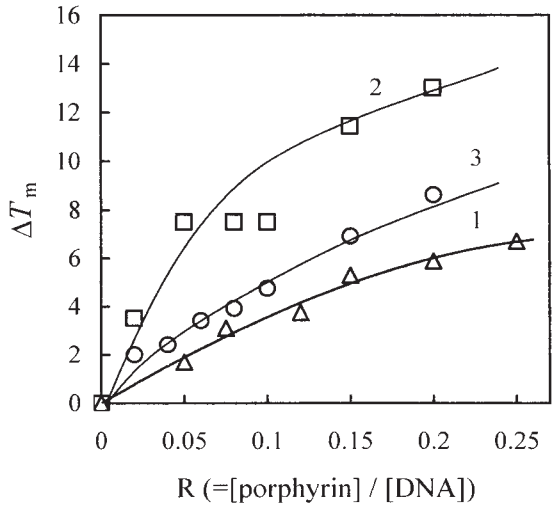

Fig. 3. Plots of the increase in melting temperature (ΔT_m) vs the molar ratio of porphyrin to CT-DNA in base pair (R). Porphyrin: (1), H_2-**1** (△); (2), Cu-**1** (□); (3), Zn-**1** (○).

Hydrodynamic methods such as viscometric measurements are some of the most critical tests for inferring the binding mode of DNA in solution, i.e. intercalation or outside groove binding. The solution viscosity of DNA is sensitive to the changes in the effective length of DNA molecules. Generally an increase in the relative viscosity is ascribed to a length increase of the double helix DNA due to intercalation. On the other hand, a decrease in the relative viscosity due to the reduction of the effective length of DNA molecules results from the bending of the double helix DNA caused by electrostatic interaction between the anion site of phosphate of DNA and the cation site of porphyrin.[31] The results of viscometric measurements in the buffer solution of CT-DNA are illustrated in Fig. 4, where the molar ratios R of H_2-**1**, Cu-**1** and Zn-**1** to

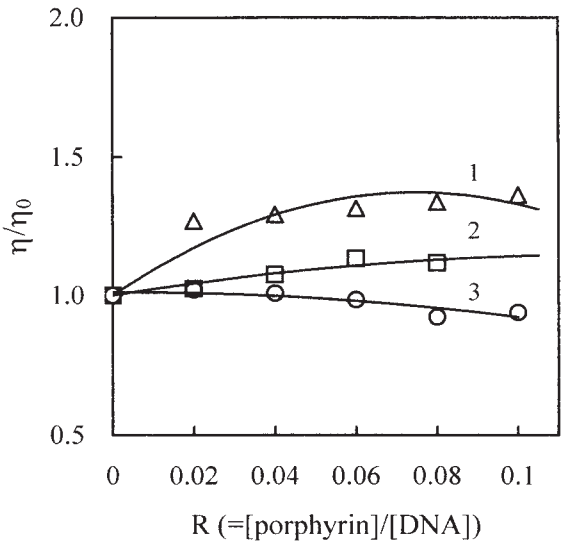

Fig. 4. Plots of the relative viscosity of CT-DNA vs the ratio R in phosphate buffer at pH 6.8 and $\mu = 0.2$ M at 30 °C. Porphyrin : (1), H_2-**1** (△); (2), Cu-**1** (□); (3), Zn-**1** (○).

CT-DNA in base pair were varied over the range of 0.01 to 0.1. For a comparative purpose, the variation of the relative viscosity with the addition of H_2-**1** to the CT-DNA buffer solution is also shown as a function of R, because metal-free H_2-**1** is already confirmed to intercalate into CT-DNA.[13] The relative viscosity of the buffer solution of CT-DNA was increased with the addition of Cu-**1**, indicating that Cu-**1** is intercalated into CT-DNA. In contrast, the relative viscosity was decreased with the addition of Zn-**1** to the buffer solution of CT-DNA, suggesting the outside binding of Zn-**1** to CT-DNA. The above viscometric consequence is consistent with the following conclusion from the visible absorption, induced CD and MCD spectra.

Spectroscopic Evidence for Metalloporphyrin–DNA Interactions. The changes in the visible absorption, induced CD and MCD spectra upon adding CT-DNA to Cu-**1** in phosphate buffer are reproduced in Fig. 5. In the presence of CT-DNA, the Soret band of Cu-**1** showed a large red shift of 10.5 nm with 43.1% substantial hypochromicity (Fig. 5a). As judged from the characteristic changes in the visible absorption spectra,[6,7] Cu-**1** is apparently intercalated into CT-DNA. The induced CD spectrum observed at $R = 0.02$ exhibited a negative peak at 396 nm and a positive peak at 413 nm. In addition, an application of the CD-mm to the induced CD spectra observed has revealed that Cu-**1** is intercalated into the 5′CG3′ step of CT-DNA.[32] The CD-mm also predicts correctly a strong positive (+) band for $\gamma = 0°$ and a strong negative (−) band for $\gamma = 90°$. The MCD spectrum of Cu-**1** showed a (+) pseudo A-term with a positive peak at 390 nm and a negative peak at 405.5 nm (Fig. 5c). In the presence of CT-DNA, the MCD spectrum of Cu-**1** shifts 8 nm to the longer wavelength and the intensity ($\Delta\varepsilon/H$) decreases 48% at $R = 0.02$, although the sign remains unchanged as the (+) pseudo A-term on going from ∞ to 0.02 in R. This change in the MCD spectra is accompanied by an increase in the excited state angular momentum (L_j), i.e. about 6.5% from 1.85 to 1.97 (deg cm^2 dmol^{-1} T^{-1}/M^{-1} cm^{-1}). In addition, the (−) induced CD band at 396 nm is well aligned with the higher energy (+) MCD band at 399.5 nm, indicating that when Cu-**1** intercalates into CT-DNA, μ_{ey} is parallel to the base pair (See the definition of μ_{ey} in Fig. 2). Moreover, the (+) induced CD band at 413 nm is well aligned with the lower energy (−) MCD band at 414 nm. Thus, the (+) induced CD band is associated with the edtm μ_{ex} of Cu-**1**, implying that when Cu-**1** intercalates into CT-DNA, μ_{ex} is perpendicular to the base pair. Consequently, upon intercalation of Cu-**1** into the 5′CG3′ step of CT-DNA, the μ_{ex} and μ_{ey} are positioned at $\gamma = 0°$ and $\gamma = 90°$, respectively.

The changes in the visible absorption, induced CD and MCD spectra upon the addition of CT-DNA to Zn-**1** in phosphate buffer are partially presented in Fig. 6. In the presence of CT-DNA, the Soret band of Zn-**1** in the visible region showed a small blue shift of 0.5 nm with 33.2% hyperchromicity at $R = 0.02$ (Fig. 6a), which is typical of outside groove binding.[6,7] The induced CD appeared as a positive band at 404.5 nm and a negative band at 439 nm (Fig. 6b). The CD-mm predicts a strong positive band and a strong negative band,[33] suggesting that Zn-**1** is bound edge-on at the 5′AT3′ step of the major groove of CT-DNA and located at a position

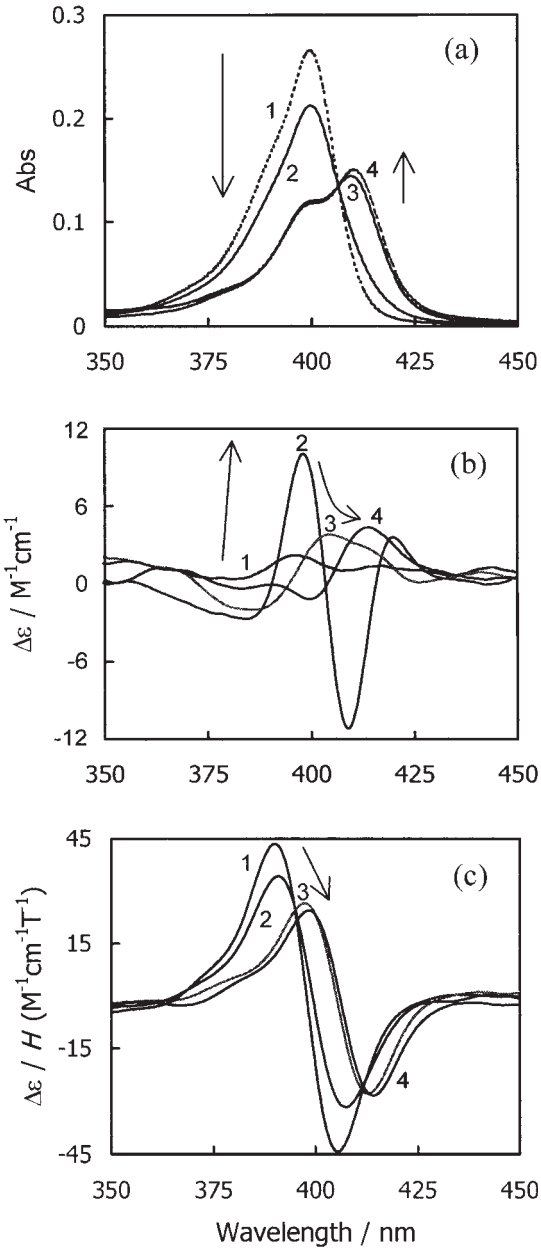

Fig. 5. Visible (a), CD (b) and MCD (c) spectra of free (dashed line) and CT-DNA-bound (solid line) Cu-**1**. The arrows indicate the direction of spectral changes and the ratio R is as follows: (1), ∞; (2), 1.0; (3), 0.1; (4), 0.02.

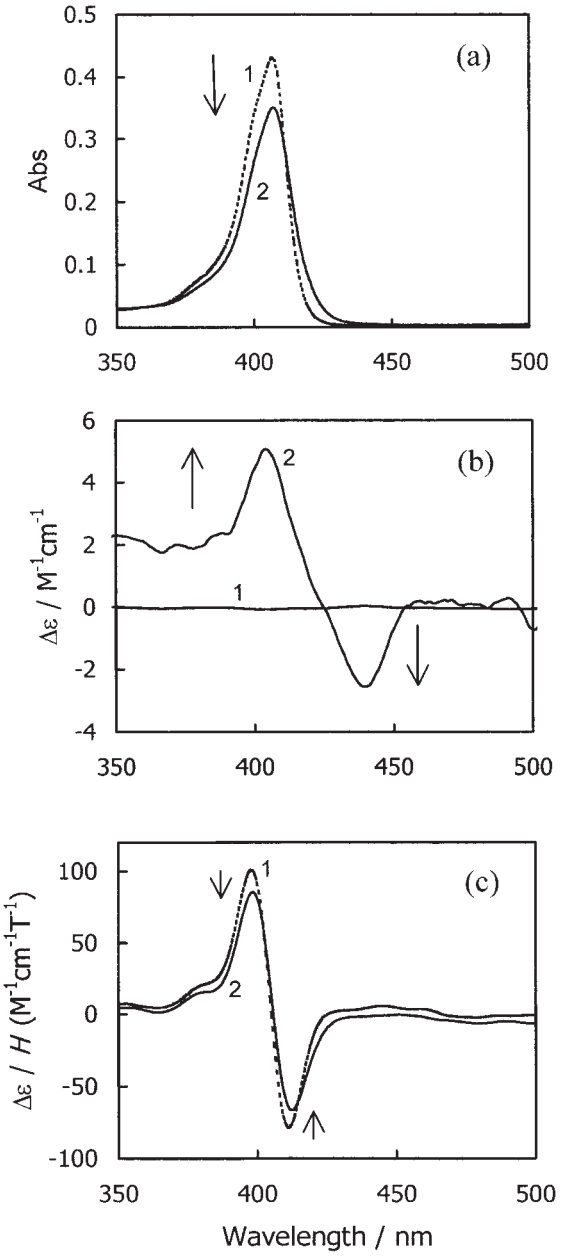

Fig. 6. Visible (a), CD (b) and MCD (c) spectra of free (dashed line) and CT-DNA-bound (solid line) Zn-**1**. The ratio R is ∞ in (1) and 0.02 in (2).

of 90°/180°/0° and 45°/180°/90° for $\alpha/\theta/\beta$ of μ_{ex} and μ_{ey}, respectively. The MCD spectrum of Zn-**1** gave a (+) pseudo A-term with a positive peak at 398 nm and a negative peak at 412 nm (Fig. 6c). In the presence of CT-DNA, the MCD spectrum of Zn-**1** shifted 0.5 nm to the shorter wavelength with a 15.3% decrease in intensity ($\Delta\mathcal{E}/H$), but the sign as the (+) pseudo A-term was maintained. The MCD spectra measured in the presence of CT-DNA have revealed that the perturbation to the localized π- and π^*-MOs ($1a_{1u}$, $3a_{2u}$ and $4e_g$) is very weak, as the change of the excited state angular momentum (L_j) increased only 0.4% from 2.65 to 2.66 (deg cm^2 dmol^{-1} T^{-1}/M^{-1} cm^{-1}). The (+) induced CD band at 404.5 nm is well aligned with the crossover of the MCD bands at 405.5 nm, indicating that Zn-**1** is perturbed homogeneously by the DNA base pairs. In other words, Zn-**1** is bound edged-on at the 5′AT3′ step of the major groove of CT-DNA probably due to the steric hindrance of the axial ligand coordinated to the central zinc(II) ion.

Binding Characteristics of Dicationic Metalloporphyrins to [poly(dG–dC)]$_2$ and [poly(dA–dT)]$_2$. The binding of Cu-**1** and Zn-**1** to double-helical synthetic DNA of the B-type [poly(dA–dT)]$_2$ and [poly(dG–dC)]$_2$ is studied in this Section to clarify interactions of dicationic metalloporphyrins with DNA by visible absorption, induced CD and MCD spectroscopy. The induced CD spectra have been interpreted in terms

of the CD matrix method, i.e. CD-mm, to assess the binding mode of the dicationic metalloporphyrin to the synthetic DNA.[32,33] All the spectroscopic data measured for the DNA binding of Cu-**1** and Zn-**1** are listed together with some assignments in Tables 1 and 2. Upon the addition of $[poly(dG–dC)]_2$ and $[poly(dA–dT)]_2$ to the phosphate buffer of Cu-**1**, the Soret band of Cu-**1** in the visible region showed a large red shift of 9.5 nm and 10.5 nm with 54.4% and 56.4% substantial hypochromicity, respectively. This is clear evidence for intercalation of dicationic Cu-**1** into both $[poly(dG–dC)]_2$ and $[poly(dA–dT)]_2$, although intercalation of tetracationic *meso*-substituted porphyrins is usually specific to the G–C base pair, like in $[poly(dG–dC)]_2$.[1] An application of the CD-mm to the induced CD spectra observed for interaction between Cu-**1** and $[poly(dG–dC)]_2$ has revealed that Cu-**1** is intercalated into the 5′CG3′ step of $[poly(dG–dC)]_2$. The CD-mm also predicts correctly a strong (+) band at 418.5 nm for $\gamma = 0^\circ$ and a strong (−) band at 401.5 nm for $\gamma = 90^\circ$. On the other hand, an application of the CD-mm to the induced CD spectra caused by interaction between Cu-**1** and $[poly(dA–dT)]_2$ predicts a strong (+) band at 413.5 nm for $\gamma = 90^\circ$, indicating that Cu-**1** is intercalated into the 5′AT3′ step of $[poly(dA–dT)]_2$. In the presence of $[poly(dG–dC)]_2$ and $[poly(dA–dT)]_2$, the MCD spectrum of Cu-**1** shifts 9 nm and 7.5 nm to the longer wavelength, and the intensity ($\Delta\varepsilon_p/H$) decreases 57.0% and 22.5%, respectively. The excited state angular momentum (L_j), i.e. $[\Delta\theta]^{p-t}/\varepsilon_{max}$, is decreased 20.5% for $[poly(dG–dC)]_2$ and increased 9.19% for $[poly(dA–dT)]_2$ from 1.85 to 1.47 and 2.02 ($deg\,cm^2\,dmol^{-1}\,T^{-1}/M^{-1}\,cm^{-1}$), suggesting that the perturbation of $[poly(dA–dT)]_2$ to the localized π- and π^*-MOs ($1a_{1u}$, $3a_{2u}$ and $4e_g$) is stronger than that of $[poly(dG–dC)]_2$. In the presence of $[poly(dG–dC)]_2$, the (−) induced CD band at 401.5 nm is well aligned with the higher energy (+) MCD band at 398 nm, implying that the intercalation of Cu-**1** into $[poly(dG–dC)]_2$ μ_{ex} is parallel to the G–C base pairs. Moreover, the (+) induced CD band at

Table 1. Spectral Data of Cu-**1** in the Presence of Synthetic DNA[a)]

Method	Parameters	Free Cu-**1**	DNA-bound Cu-**1**	
			$[Poly(dG–dC)]_2$	$[Poly(dA–dT)]_2$
Visible	λ_o/nm	400.0	409.5	410.5
	$\varepsilon_{max}/cm^{-1}\,M^{-1} \times 10^5$	1.56	0.715	0.979
	Hypochromicity/%	—	54.4	56.4
	D_{aj}/Debye^2	90.4	21.9	39.8
CD	λ_o/nm	—	401.5; 418.5	413.5
	$\Delta\varepsilon/cm^{-1}\,M^{-1}$	—	−9.20; +3.57	+7.32
	$R_{aj} \times 10^3$, Debye μ_B	—	−78.1; +16.7	+56.4
MCD	$\lambda_{crossover}$/nm	398.0	407.0	405.5
	λ_p/nm	390.0	398.0	398.0
	$\Delta\varepsilon_p$/H, $cm^{-1}\,M^{-1}\,T^{-1}$	+43.5	+18.7	+33.7
	λ_t/nm	405.5	415.0	413.5
	$\Delta\varepsilon_t$/H, $cm^{-1}\,M^{-1}\,T^{-1}$	−44.2	−13.1	−33.0
	$\Delta[\theta]^{p-t}/\varepsilon_{max}$, $deg\,cm^2\,dmol^{-1}\,T^{-1}/M^{-1}\,cm^{-1}$	1.85	1.47	2.02

a) In phosphate buffer of pH 6.8 and $\mu = 0.2$ M and at $R = 0.02$. p and t are peak and trough, respectively. $\Delta[\theta] = \Delta\varepsilon \times 3300$.[34]

Table 2. Spectral Data of Zn-**1** in the Presence of Synthetic DNA[a)]

Method	Parameters	Free Zn-**1**	DNA-bound Zn-**1**	
			$[Poly(dG–dC)]_2$	$[Poly(dA–dT)]_2$
Visible	λ_o/nm	406.0	406.5	407.0
	$\varepsilon_{max}/cm^{-1}M^{-1} \times 10^5$	2.24	2.07	1.58
	Hypochromicity/%	—	−13.3	−35.4
	D_{aj}/Debye^2	95.7	90.9	81.9
CD	λ_o/nm	—	404.5; 425.0	416.0
	$\Delta\varepsilon/cm^{-1}\,M^{-1}$	—	+2.73; −3.59	+10.7
	$R_{aj} \times 10^3$, Debye μ_B	—	+10.3; −31.1	+288
MCD	$\lambda_{crossover}$/nm	405.0	405.5	408.0
	λ_p/nm	398.0	398.5	399.5
	$\Delta\varepsilon_p$/H, $cm^{-1}\,M^{-1}\,T^{-1}$	+101	+77.2	+69.9
	λ_t/nm	411.0	412.0	416.0
	ε_t/H, $cm^{-1}\,M^{-1}\,T^{-1}$	−78.9	−58.6	−54.4
	$\Delta[\theta]^{p-t}/\varepsilon_{max}$, $deg\,cm^2\,dmol^{-1}\,T^{-1}/M^{-1}cm^{-1}$	2.65	2.16	2.60

a) In phosphate buffer of pH 6.8 and $\mu = 0.2$ M and at $R = 0.02$. p and t are peak and trough, respectively. $\Delta[\theta] = \Delta\varepsilon \times 3300$.[34]

418.5 nm is well aligned with the lower energy (−) MCD band at 415 nm. The (+) induced CD band is associated with the edtm μ_{ey} of Cu-**1** and thus, when Cu-**1** intercalates into [poly(dG–dC)]$_2$, μ_{ey} is perpendicular to the G–C base pairs. In the presence of [poly(dA–dT)]$_2$, the (+) induced CD band at 413.5 nm is very well aligned with the lower energy (−) MCD band at 413.5 nm, indicating that when Cu-**1** intercalates into [poly(dA–dT)]$_2$, μ_{ex} is parallel to the A–T base pairs. As a result, it has been demonstrated that dicationic Cu-**1** intercalates into such kinds of synthetic DNA as [poly(dG–dC)]$_2$ and [poly(dA–dT)]$_2$ in a similar fashion.

The Soret band of Zn-**1** in the presence of [poly(dG–dC)]$_2$ and [poly(dA–dT)]$_2$ showed a small blue shift of 0.5 nm and 1 nm with 13.3% and 35.4% hyperchromicity, respectively (Table 2). These spectral features are typical of outside groove binding,[6,7] indicating that Zn-**1** is outside bound to [poly(dG–dC)]$_2$ and [poly(dA–dT)]$_2$. In the presence of [poly(dG–dC)]$_2$, the induced CD spectra appeared as a positive band at 404.5 nm and a negative band at 425 nm. The CD-mm predicts a strong negative band and a strong positive band, and thus Zn-**1** is bound edge-on at the 5′CG3′ step of the major groove of [poly(dG–dC)]$_2$ at a position of 90°/180°/0° and 45°/180°/90° for $\alpha/\theta/\beta$ of μ_{ex} and μ_{ey}, respectively. In the presence of [poly(dA–dT)]$_2$, the induced CD spectra appeared only as a positive band at 416 nm. The CD-mm predicts a strong positive band, suggesting that Zn-**1** is bound edge-on at the 5′TA3′ step of the minor groove of [poly(dA–dT)]$_2$ and situated at a position of 45°/0°/90° and 90°/0°/0° for $\alpha/\theta/\beta$ of μ_{ex} and μ_{ey}, respectively. In the presence of [poly(dG–dC)]$_2$ and [poly(dA–dT)]$_2$, the MCD spectra of Zn-**1** shift 0.5 and 3 nm to the longer wavelength, and the intensity ($\Delta\varepsilon_p/H$) decreases 23.6 and 30.8%, respectively. In addition, the excited state angular momentum (L_j), i.e. $[\Delta\theta]^{p-t}/\varepsilon_{max}$ decreases 18.5 and 2.9% on going from 2.65 to 2.16 and 2.60 (deg cm^2 dmol^{-1} T^{-1}/M^{-1} cm^{-1}), indicating that the perturbation of [poly(dG–dC)]$_2$ to the localized π- and π^*-MOs ($1a_{1u}$, $3a_{2u}$ and $4e_g$) is stronger than that of [poly(dA–dT)]$_2$. The (+) induced CD band at 404.5 nm in the presence of [poly(dG–dC)]$_2$ is well aligned with the crossover of the MCD band at 405.5 nm, implying that Zn-**1** receives a homogeneous perturbation. The (+) induced CD band at 416 nm in the presence of [poly(dA–dT)]$_2$ is very well aligned with the lower energy (−) MCD band at 416 nm, suggesting that when Zn-**1** is outside bound to [poly(dA–dT)]$_2$, μ_{ex} is almost perpendicular to the A–T base pairs. From these results, it has been shown that dicationic Zn-**1** is outside bound to both [poly(dG–dC)]$_2$ and [poly(dA–dT)]$_2$ but in a different manner.

Effect of Central Metal Ions on Affinity and Selectivity. The strength of interaction of porphyrins with DNA is associated with the binding constant which is used to determine how strongly porphyrins interact with DNA in a buffer solution. The apparent binding constant (K_{app}) is calculated from the changes in the visible absorption spectra accompanied by the addition of DNA to porphyrins in the phosphate buffer at pH 6.8 and $\mu = 0.2$ M.[27–29] In the previous paper, the binding constant of H_2-**1** was reported to be 10^5–10^7 M^{-1} and comparable to that of other well-known porphyrin intercalators.[13] This high affinity of H_2-**1** to DNA is clearly due to the naked *meso*-position of the dicationic bis(imidazoliumyl)porphyrin, and thus the π-electron system of H_2-**1** gives rise to the extension of the effective hydrophobic site. In comparison with the free-base porphyrin, the binding constant of the metalloporphyrin depends on the kind of central metal ions (cf. Table 3). The affinity of the dicationic bis(imidazoliumyl)porphyrinatometal studied in this work to DNA can be evaluated by means of the K_{app} values. The binding constant of intercalative Cu-**1** is in the order of 10^6 M^{-1}, while the K_{app} of outside binding Zn-**1** is in the order of 10^4 M^{-1}. A comparison of these results has revealed that the affinity of the dicationic bis(imidazoliumyl)porphyrinatometal to DNA is not always larger than that of the corresponding free-base bis(imidazoliumyl)porphyrin, although the intercalator Cu-**1** has a larger affinity than the outside binder Zn-**1**.

From a comparison of K_{app} in Table 3, it is shown that the selectivity of the metalloporphyrins to DNA base pairs depends on their central metal ions. The K_{app} of Zn-**1** to [poly(dA–dT)]$_2$ is larger than that to [poly(dG–dC)]$_2$ and thus Zn-**1** is selective to the A–T-rich sites. On the other hand, the K_{app} of Cu-**1** is almost independent of the kind of DNA, although it is known that the tetracationic copper(II) complex of *meso*-tetrakis(methylpyridiniumyl)porphyrin is selective to the G–C-rich sites.[1,2] In fact, Cu-**1** intercalates into both A–T and G–C base pairs to increase the molecular size of DNA. The effect of the central metal ion on the affinity and selectivity of dicat-

Table 3. Thermodynamic Parameters of Interactions between Porphyrin and DNA[a)]

Porphyrin	DNA	$K_{app}/10^5$	ΔG^0	ΔH^0	ΔS^0 ($-T\Delta S$)	Ref.
H_2-**1**	CT-DNA	22.6	−36.2	−34.2	+6.70 (−2.00)	13
	[poly(dA–dT)]$_2$	103	−40.0	−106	−222 (+66.1)	
	[poly(dG–dC)]$_2$	2.70	−31.0	−39.0	−27.2 (+8.11)	
Cu-**1**	CT-DNA	16.9	−35.5	−6.98	+95.7 (−28.5)	This work
	[poly(dA–dT)]$_2$	13.5	−35.0	+8.01	+144 (−42.9)	
	[poly(dG–dC)]$_2$	16.8	−35.5	−22.2	+45.1 (−16.4)	
Zn-**1**	CT-DNA	0.988	−22.8	−3.45	+65.0 (−19.4)	This work
	[poly(dA–dT)]$_2$	2.17	−24.7	−5.92	+63.2 (−18.8)	
	[poly(dG–dC)]$_2$	0.660	−21.8	−38.1	−54.9 (+16.4)	

a) K_{app} (M^{-1}) is the apparent binding constant of porphyrin–DNA interactions in the phosphate buffer at pH 6.8 and $\mu = 0.2$ M at 25 °C and calculated from the average of three nearest values. ΔG^0 (kJ mol^{-1}), ΔH^0 (kJ mol^{-1}), ΔS^0 (J K^{-1} mol^{-1}) and $-T\Delta S$ (kJ mol^{-1}) were calculated at 25 °C.

ionic metalloporphyrins to DNA is summarized as follows. First, Cu-**1** has a higher affinity to DNA than Zn-**1** probably due to the difference in the binding mode. As described above, Cu-**1** is intercalated into any kind of DNA, while Zn-**1** is outside bound to DNA. It is noteworthy that the insertion of metal ions into dicationic porphyrins affects the binding mode and affinity of the porphyrins to DNA. Second, the K_{app} of H_2-**1** to [poly(dA–dT)]$_2$ is about 40 times larger than that to [poly(dG–dC)]$_2$, clearly suggesting that H_2-**1** is selective to the A–T base pair. However, upon metalation of H_2-**1**, Zn-**1** becomes less selective to the A–T base pair, while Cu-**1** has much the same selectivity to every kind of DNA. Thus, the insertion of metal ions into H_2-**1** leads to a decrease in selectivity of the dicationic porphyrin to the base pair. Interestingly, it was reported that CuTMPyP has selectivity to G–C rich sites, while ZnTMPyP is selective to A–T rich sites.[14,15] It has been confirmed that the binding mode can be controlled by insertion of metal ions into dicationic porphyrins having only two *meso*-substituents, although their selectivity to the base pair will be lowered or lost.

Influence of Central Metal Ions on Thermodynamic Properties. An understanding of the driving force of interactions between porphyrin and DNA provides some information about the binding properties of metalloporphyrins to DNA. The thermodynamic parameters of the interaction of dicationic metalloporphyrins with DNA were obtained by determining the binding constants at various temperatures. In the temperature range of 18 to 39 °C, the van't Hoff plots are linear, indicating that the thermodynamic parameters such as ΔH and ΔS are constant in this temperature range. Therefore, the values for ΔG, ΔH and ΔS serve as the thermodynamic parameters of metalloporphyrin–DNA interactions (Table 3). The free energy changes in the binding of H_2-**1** to [poly(dA–dT)]$_2$ are the negatively largest of those to synthetic and native DNA. In contrast, the free energy changes in the binding of Cu-**1** are almost the same magnitude for all the DNA. The interaction of the porphyrins with DNA should be strong, when the standard free energy change (ΔG^o) is negatively large. As already reported, the binding of H_2-**1** to CT-DNA, [poly(dA–dT)]$_2$ and [poly(dG–dC)]$_2$ is exothermic and enthalpically driven.[13] On the other hand, the binding of Cu-**1** and Zn-**1** to CT-DNA, [poly(dA–dT)]$_2$ and [poly(dG–dC)]$_2$ is different from that of the corresponding free-base porphyrin. It is exothermic and entropically driven except for the binding of Cu-**1** to [poly(dA–dT)]$_2$. This exceptional feature in Cu-**1** can be explained by the nature of polynucleotides specifically, because the G–C and A–T base pairs in the B-type DNA are accompanied by almost the same number of water molecules per base pair.[35] For one thing, the spine of water molecules runs along with the minor groove in the long A–T sequence to stabilize the special conformation.[36] For another, the unusual intercalation of Cu-**1** into [poly(dA–dT)]$_2$ might flip the base pair out of the double-helical DNA to break two hydrogen bonds between the A–T base pair,[8] and lead to a positive enthalpy change with a relatively large entropy change. As a result, the interaction of dicationic Cu-**1** with [poly(dA–dT)]$_2$ would be an endothermic reaction and bring about the positive enthalpy change.

Upon the interaction of Cu-**1** and Zn-**1** with DNA, the enthalpy changes ΔH are less exothermic than those in the free-base porphyrin. In other words, the less exothermic enthalpy changes will lead to the relatively large $T\Delta S$ term to contribute to the large negative free energy changes. It is well-known that the Coulombic interaction between cation and anion is driven by positive entropy changes.[37] Therefore, the positive entropy changes upon the binding of the dicationic metalloporphyrin to DNA must come mainly from the electrostatic interaction between positively charged *meso*-substituents and negatively charged phosphate oxygens. Upon closer contact or interaction between these charged groups, the water molecules bound to these ionic groups are released and the positive translational entropy would induce the positive entropy changes in the overall thermodynamics of metalloporphyrin–DNA interactions. In the case of the binding of Cu-**1** to [poly(dA–dT)]$_2$, desolvation which occurs in the ionic interaction is significantly observed, as shown by the positive enthalpy changes.

The insertion of a central metal ion into porphyrin affects the enthalpy changes because the central metal ion of the metalloporphyrin may be coordinated by the ring-nitrogen of base pairs or the carbonyl group of thymine. This kind of coordination interaction has been observed for ZnTMPyP and CoTMPyP,[38] and CuTMPyP.[39] In addition, the interaction of the metalloporphyrin with DNA gives rise to a large distortion in the structure of DNA compared with that of the metal-free porphyrin.[8] Such a distortion results in the change in the local charge density, which undergoes the condensed counter-ion release from the interacting surface. Both distortion of DNA and condensed counter-ion release are associated with large positive entropy changes.[40] Consequently, the endothermic enthalpy changes in desolvation from the site of metal coordination bring about more positive entropy changes in the dicationic metalloporphyrin than in the corresponding free-base porphyrin. The binding process of dicationic porphyrins to DNA is driven enthalpically in the metal-free porphyrin but entropically in the metalloporphyrin. The insertion of metal ions into H_2-**1** conclusively influences the thermodynamic driving force of porphyrin–DNA interactions.

Conclusion

The copper(II) complex Cu-**1** intercalates into every kind of DNA, but in a manner different from that of metal-free H_2-**1** to lose the base-pair selectivity observed for H_2-**1**. In contrast, the zinc(II) complex Zn-**1** is outside bound edge-on to every kind of DNA due to the influence of axial ligands. The binding process of Cu-**1** and Zn-**1** to DNA is still exothermic, although the enthalpy changes are smaller than those of H_2-**1**. The entropy changes in the binding of Cu-**1** and Zn-**1** to DNA are large and positive compared with those of H_2-**1**. The binding interaction of H_2-**1** to DNA is enthalpically driven, while it is entropically driven upon insertion of the central metal ion. These results have demonstrated that insertion of the transition metal ion changes the nature of DNA binding and the kind of the central metal ion affects the binding mode of the dicationic metalloporphyrin to the double helix DNA.

This work was supported in part by a Grant-in-Aid for Sci-

entific Research (No. 13554025) from the Ministry of Education, Culture, Sports, Science and Technology. The second author (D. H. T.) acknowledges financial support from The Hitachi Scholarship Foundation, Tokyo, Japan through Research Fellowship Program.

References

1 L. G. Marzilli, *New J. Chem.*, **14**, 409 (1990).
2 R. F. Pasternack and E. J. Gibbs, *Met. Ions Biol. Syst.*, **33**, 367 (1996), and references therein.
3 G. Valduga, B. Breda, G. M. Giacometti, G. Jori, and E. Reddi, *Biochem. Biophys. Res. Commun.*, **256**, 84 (1999).
4 S. Mettath, B. R. Munson, and R. K. Pandey, *Bioconjugate Chem.*, **10**, 94 (1999).
5 V. S. Chirvony, V. A. Galievsky, S. N. Terekhov, B. M. Dzhagarov, V. V. Ermolenkov, and P. Turpin, *Biospectroscopy*, **5**, 302 (1999).
6 N. E. Makundan, G. Petho, D. W. Dixon, and L. G. Marzilli, *Inorg. Chem.*, **34**, 3677 (1995).
7 A. B. Guliaev and N. B. Leontis, *Biochemistry*, **38**, 15425 (1999).
8 L. A. Lipscomb, F. X. Zhou, S. R. Presnell, R. J. Woo, M. E. Peek, R. R. Plaskon, and L. D. Williams, *Biochemistry*, **35**, 2818 (1996).
9 R. K. Wall, A. H. Shelton, L. C. Bonaccorsi, S. A. Bejune, D. Dubé, and D. R. McMillin, *J. Am. Chem. Soc.*, **123**, 11480 (2001).
10 R. J. Fiel, *J. Biomol. Struct. Dyn.*, **6**, 1259 (1989).
11 R. F. Pasternack and E. J. Gibbs, *ACS Symp. Ser.*, **402**, 59 (1989).
12 D. H. Tjahjono, T. Akutsu, N. Yoshioka, and H. Inoue, *Biochim. Biophys. Acta*, **1472**, 333 (1999).
13 D. H. Tjahjono, T. Yamamoto, S. Ichimoto, N. Yoshioka, and H. Inoue, *J. Chem. Soc., Perkin Trans. 1*, **2000**, 3077.
14 N. R. Barnes and A. F. Schreiner, *Inorg. Chem.*, **37**, 6935 (1998).
15 F. Qu and N. Q. Li, *Electroanalysis*, **17**, 1348 (1997).
16 D. L. Banville, L. G. Marzilli, J. A. Strickland, and W. D. Wilson, *Biopolymers*, **25**, 1837 (1986).
17 T. A. Gray, K. T. Yue, and L. G. Marzilli, *J. Inorg. Biochem.*, **41**, 205 (1991).
18 R. D. Well, J. E. Larson, R. C. Grant, B. E. Shortle, and C. R. Cantor, *J. Mol. Biol.*, **54**, 465 (1970).
19 W. Muller and D. M. Crothers, *J. Mol. Biol.*, **35**, 251 (1968).
20 D. E. V. Schmechel and D. M. Crothers, *Biopolymers*, **10**, 465 (1971).
21 C. J. Weiss, *J. Mol. Spectrosc.*, **44**, 37 (1972).
22 R. Lyng, A. Rodger, and B. Nordén, *Biopolymers*, **31**, 1709 (1991).
23 R. Lyng, A. Rodger, and B. Nordén, *Biopolymers*, **32**, 1201 (1992).
24 R. Lyng, T. Härd, and B. Nordén, *Biopolymers*, **26**, 1327 (1987).
25 M. Kubista, B. Akerman, and B. Nordén, *J. Phys. Chem.*, **92**, 2352 (1988).
26 N. R. Barnes, A. F. Schreiner, M. G. Finnegan, and M. K. Johnson, *Biospectroscopy*, **4**, 341 (1998).
27 A. M. Pyle, J. P. Rehman, R. Meshoyrer, C. V. Kumar, N. J. Turro, and J. K. Barton, *J. Am. Chem. Soc.*, **111**, 3051 (1989).
28 J. Onuki, A. V. Ribsa, M. H. G. Mederios, K. Araki, H. E. Toma, L. H. Catalani, and P. D. Mascio, *Photochem. Photobiol.*, **63**, 272 (1996).
29 S. Routier, V. Joanny, A. Zaparucha, H. Vezin, J. P. Chatteau, J. L. Bernier, and C. Bailly, *J. Chem. Soc., Perkin Trans. 2*, **1998**, 863.
30 R. J. Fiel, J. C. Howard, E. H. Mark, and N. Datta-Gupta, *Nucleic Acids Res.*, **6**, 3093 (1979).
31 L. G. Marzilli, G. Petho, M. Lin, M. S. Kim, and D. W. Dixon, *J. Am. Chem. Soc.*, **144**, 7575 (1992).
32 Conventionally the most reasonable position of Cu-**1** between $[poly(dG–dC)]_2$ is read on the counter maps of Induced Rotatory Strength (IRS) in Ref. 22 by using the intensity and sign of induced CD signals experimentally measured.
33 On the IRS counter maps of Ref. 23, the geometric parameters α, β and θ and the orientation of the electric dipole transition moment μ_e are estimated from the induced CD-spectral data (see also Fig. 2).
34 P. J. Stephens, W. Suëtaak, and P. N. Schatz, *J. Chem. Phys.*, **44**, 4592 (1966).
35 N. R. Barnes, A. F. Schreiner, and M. A. Dolan, *J. Inorg. Biochem.*, **72**, 1 (1998).
36 M. Feig and B. M. Pettitt, *Biopolymers*, **48**, 199 (2000).
37 W. Saenger, "Principles of Nucleic Acids Structure," ed by C. R. Cantor, Springer-Verlag, New York (1984), Ch. 17, p. 368.
38 H. Ogoshi, T. Mizutani, T. Hayashi, and Y. Kuroda, "The Porphyrin Handbook," ed by K. M. Kadish, K. M. Smith, and R. Guilard, Academic Press, San Diego (1999), Vol. 6, Ch. 46, p. 279.
39 V. Galievsky, V. Chirvony, V. Ermolenkov, S. Kruglik, P. Mojzes, and P. Y. Turpin, "Spectroscopy of Biological Molecules: Modern Trends," ed by P. Carmona, R. Navarro, and H. Hernanz, Kluwer Academic Publishers, Netherlands (1997), p. 351.
40 J. B. Chaires, *Biopolymers*, **44**, 201 (1997).